Electron Microscopic Analysis of Heterogeneous Precipitates in Hastelloy C-276

M. RAGHAVAN, B. J. BERKOWITZ, and J. C. SCANLON

Three distinct second phases were observed to form heterogeneously at grain and deformation twin boundaries when Hastelloy C-276 was aged in the temperature range of 923 to 1173 K. The most abundant was the faulted, molybdenum rich μ phase. The next most abundant phase was molybdenum rich M_6C carbides, and the third phase, which was observed very infrequently, was tentatively identified as the P phase. The compositions of these phases were remarkably similar, and the need to employ several electron microscopy techniques is emphasized. The origin of the μ phase is discussed in the light of its chemistry.

I. INTRODUCTION

THE present investigation was conducted to characterize the second phase particles in Hastelloy C-276* using an analytical scanning transmission electron microscope in order to understand their effect on the mechanical and stress corrosion properties of the alloy. Investigation in our laboratory[1] and previous published reports[2-9] have identified two types of precipitation reactions in this alloy. At temperatures in the range of 573 to 923 K, the alloy precipitates an ordered phase of the type $Ni_2(Cr,Mo)$.[1,10-13] This precipitation reaction is homogeneous with no preferential precipitation at the grain boundaries or twin boundaries.[1] At temperatures above 923 K, several precipitate phases were observed to nucleate heterogeneously at the twin and grain boundaries. Using X-ray diffraction techniques, these precipitates were previously identified as the μ, M_6C, and P phases.[2-9]

*Trademark, Cabot Corporation, Kokomo, Indiana.

μ phase has been reported to form in Fe-Mo and Fe-W binary systems with an A_7B_6 stoichiometry.[14] It has a hexagonal crystal structure (a = 4.76Å, c = 25.72Å) with a rhombohedral symmetry, and was found to form in several commercial nickel and iron based alloys. M_6C carbide forms in alloy systems containing Mo or W in excess of about six pct,[15] and the metal content of the carbide is largely Mo and/or W. The carbide has a diamond cubic crystal structure ($a \simeq$10.8 to 11.2Å), and its lattice parameter is close to the chromium rich $M_{23}C_6$ carbide which has a face centered cubic crystal structure ($a \simeq$10.6Å). The P phase was originally identified by Rideout *et al*,[16] and Bloom and Grant[17] in the Ni-Cr-Mo system and was recently reported to have a tetragonal crystal structure.[14] This phase was found to coexist with the sigma phase in the Ni-Cr-Mo system[16] and the μ and δ phases in the Fe-Ni-Mo ternary system.[14]

The present investigation was carried out to determine the composition and crystal structure of the second phase particles in Hastelloy C276. This article describes the characterization of these precipitates using the X-ray microanalysis and microdiffraction techniques. The effect of these precipitation reactions on stress corrosion cracking will be described in a subsequent publication.

M. RAGHAVAN, B. J. BERKOWITZ, and J. C. SCANLON are all with Corporate Research Science Laboratories, Exxon Research and Engineering Company, P. O. Box 45, Linden, NJ 07036.

Manuscript submitted July 22, 1981.

II. EXPERIMENTAL PROCEDURE

Cold rolled samples (37 pct) of the alloy were aged in the range of 923 to 1173 K for times up to 1000 hours, and thin samples for electron microscopy were prepared by conventional electropolishing and subsequent ion thinning. The samples were examined in an EM400T electron microscope with X-ray energy dispersive analytical capability. The sample thickness, measured by the conventional contamination mark method, ranged from 1000 to 1500Å. Quantitative chemical analysis was obtained by the thin foil ratio method,[18] and absorption effects were analyzed and corrected using the procedure described by Goldstein *et al*.[19] The k values used in the analysis were experimentally determined using independent standards[20] and are listed in Table I. In order to double check the accuracy of the k ratios used in the quantitative analysis, the average composition of the sample was measured from X-ray spectra generated from several grains of the unaged thin sample using an approximately 5 μm beam to average any possible local variations in composition. The table also shows the chemical analysis supplied by the manufacturer and the agreement between the analysis was excellent, indicating that the accuracy of the k ratios used in the analysis was better than 10 pct. Second phase particles from selected samples were electrolytically extracted in a 10 pct perchloric-methanol solution at 25 V and 300 K, centrifuged and subjected to microanalysis. These results compared very well with the analysis of the same particles in the thin sample within the errors indicated in the particle analyses (Table II).

Table I. Composition of Hastelloy C-276, Wt Pct

Element	Chemical Analysis*	X-Ray Micro-analysis ($\pm\sigma$)**	k[20]
Ni	57.0	56.6 (0.7)	1.29
Mo	15.6	15.3 (0.9)	1.43
Cr	15.06	15.9 (0.30)	1.231
Fe	6.4	6.6 (0.20)	1.27
W	3.76	4.2 (0.4)	2.24
Co	2.18	1.7 (0.2)	1.36

*Supplied by manufacturer: other elements are: C-0.0002; P-0.011; S < 0.002; V-0.17; Mn-0.04 and Si-0.04.

**Take off angle: 20 deg, specimen tilt: 0 deg, M line for W, L line for Mo, K lines for all other elements.

ISSN 0360-2133/82/0611-0979$00.75/0

Table II. X-Ray Microanalysis of Second Phase Particles

Element	Composition, Wt Pct ($\pm\sigma$)		
	μ	M_6C	P
Ni	28.0 (2.4)	27.0 (1.7)	27.9
Mo	49.5 (2.2)	47.5 (1.8)	48.0
Cr	11.0 (0.4)	14.3 (0.9)	13.3
W	7.5 (2.6)	5.0 (2.7)	4.0
Fe	2.0 (0.2)	2.1 (0.1)	4.9
Co	1.5 (0.1)	1.5 (0.1)	1.7
C	0.002*	2.6**	——
V	0.1 (0.05)	0.3 (0.05)	——

*Alloy carbon content
**Calculated for M_6C

Final sample preparation of coarse particles by ion beam thinning for X-ray microanalysis (approximately 0.2 to 1.0 μm in size) was found to be very suitable because ion thinning provided uniformly thin particles so that particle thicknesses could be easily and accurately measured for the absorption correction. If these coarse particles are extracted for analysis or if thin samples were made only by conventional electropolishing, the particles retain their original shape and size from the bulk sample. In such case, the particle thicknesses were generally large and nonuniform and accurate quantitative microanalysis cannot be conducted. Hence, samples after ion thinning were used for all the microanalyses in the present investigation.

III. RESULTS

The unaged sample of the alloy showed essentially a single-phase austenite structure. Upon aging the sample in the temperature range of 923 to 1173 K, the precipitates nucleated heterogeneously at the grain and deformation twin boundaries (Figure 1). The volume fraction and the size of the precipitates increased with aging time at each aging temperature. The size of the particles ranged from 500Å at early stages of aging (five to 15 minutes) to about 1 μm after prolonged aging. The chemistry and crystal with aging temperature or time, and the results described below are valid for all the aging conditions examined in the present investigation. Three distinct precipitates were identified by electron diffraction and X-ray microanalysis. The μ phase precipitates were the most abundant, followed by M_6C carbide precipitates. The precipitate which was less frequently observed was tentatively identified as the P phase.

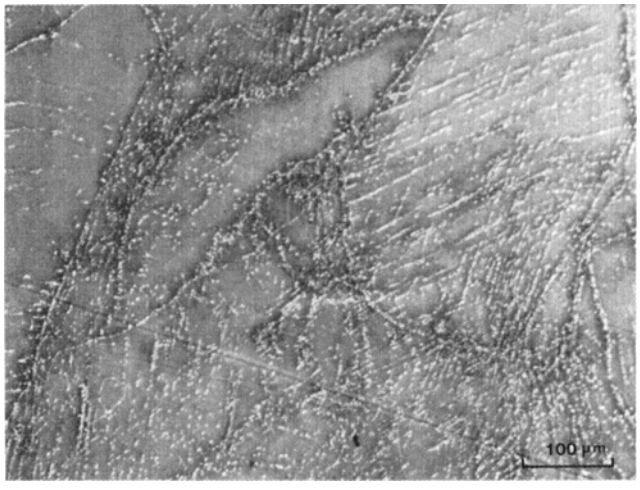

Fig. 1 — Scanning electron micrograph of a sample aged at 1173 K/60 s showing grain and deformation twin boundary precipitation.

Figure 2 shows a bright field image of a μ phase particle. X-ray microanalysis of the particles is shown in Table II and, as suggested previously, they are enriched in Mo and W.[2-9] These particles contained numerous planar faults, and diffraction analysis showed that the faults formed on the basal planes of the particle. The fault density, however, varied from particle to particle. The faulting is characteristic of the μ phase and can be used as a distinguishing feature to identify the μ phase from other precipitates in the sample. An electron diffraction map of a μ phase particle is shown in Figure 3. The diffraction patterns were indexed for the rhombohedral symmetry where the allowed reflections are $\bar{h} + k + 1 = 3n$. Streaking along the $[001]\mu$ direction was observed due to faults in the particles (Figure 4). The streaks were strong in the first and second rows of reflections along $[001]\mu$, while in the row containing the transmitted beam and in the third row, the intensity of streaking was very weak. This nonuniform intensity streaking indicates that the streaks are not due to shape factor alone.

The next abundant second phase particles were the M_6C carbides. At all the aging temperatures the carbide particles nucleated rapidly prior to the formation of μ phase, were generally elongated, and did not contain any faults. X-ray microanalysis results from the carbides are shown in Table II. It is interesting to note that the metal composition of the carbide is very similar to the composition of the μ phase except the chromium level in the carbide was higher. This is clearly shown in Figure 5 which shows superimposed X-ray spectra from the carbide and μ phase. To confirm that the particles contain carbon, energy loss spectrum from the thin edge of a carbide particle was generated. The spectrum shown in Figure 6 clearly showed the carbon K edge at 285 eV. Energy loss spectra were also generated from the adjacent matrix regions to check if the observed carbon edge in the carbide could be due to contamination. Spectra from the matrix did not show any carbon. A microdiffraction map of the M_6C carbide particles is shown in Figure 7. It is difficult to distinguish the M_6C carbides from the $M_{23}C_6$ carbides by electron diffraction except in the [001] orientation (Figure 8). The (200) type reflections which are kinematically forbidden in the diamond cubic structure appear

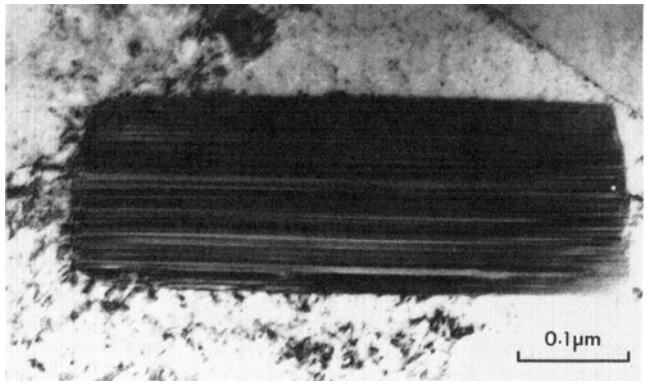

Fig. 2 — Bright field image of a μ phase particle showing extensive faulting.

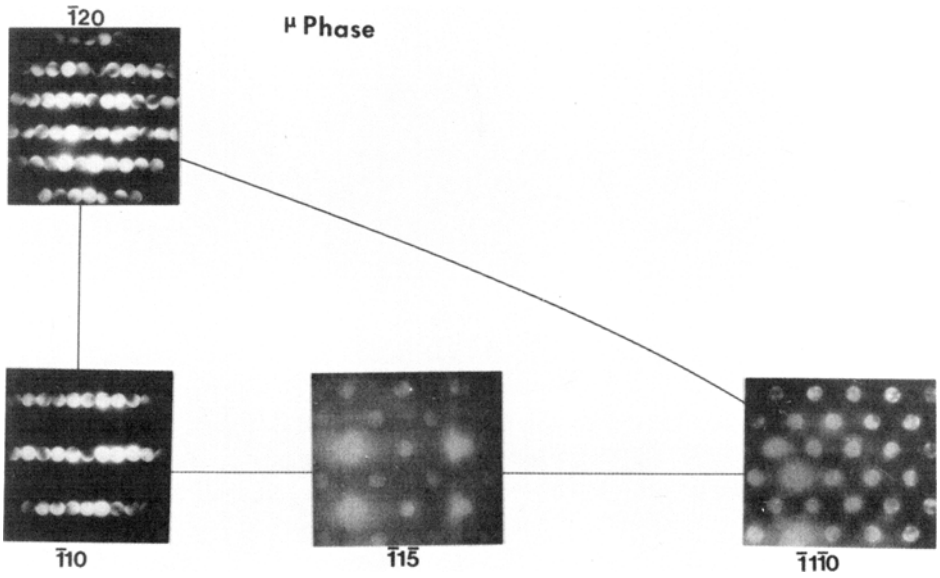

Fig. 3 — Zone axis map of the μ phase.

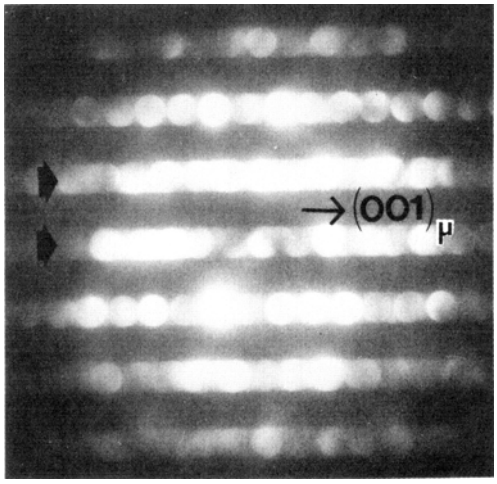

Fig. 4 — A [010] microdiffraction pattern from the μ phase showing strong streaking in the first and second rows (arrows) and weak streaking in the zero and third rows.

due to double diffraction in many of the lower symmetry orientations such as [112] and [$0\bar{1}1$] shown in Figure 7. The Zero Order Laue Zone (ZOLZ) in Figure 8 shows a square mesh of (220), ($2\bar{2}0$), and (400) reflections, and the (200) type reflections do not appear due to absence of double diffraction routes in the Zero Layer. However, in the First Order Laue Zone (FOLZ) the reflection corresponding to {200} are allowed. This is illustrated by two reflections in the FOLZ, (23,1,1) and (23,3,1), both of which are allowed and are separated by the (020) reciprocal lattice vector. Hence, these additional spots are observed in the FOLZ. These reflections could cause double diffraction resulting in weak intensities in the (200) type positions in the ZOLZ and is marked by an arrow. In the case of the $M_{23}C_6$ carbide, the (200) type reflections are allowed in the ZOLZ and hence, no additional reflections appear in the FOLZ. Thus, the M_6C carbide can be easily distinguished from the $M_{23}C_6$ carbide in the [001] orientation. These effects have been reported recently.[21,22]

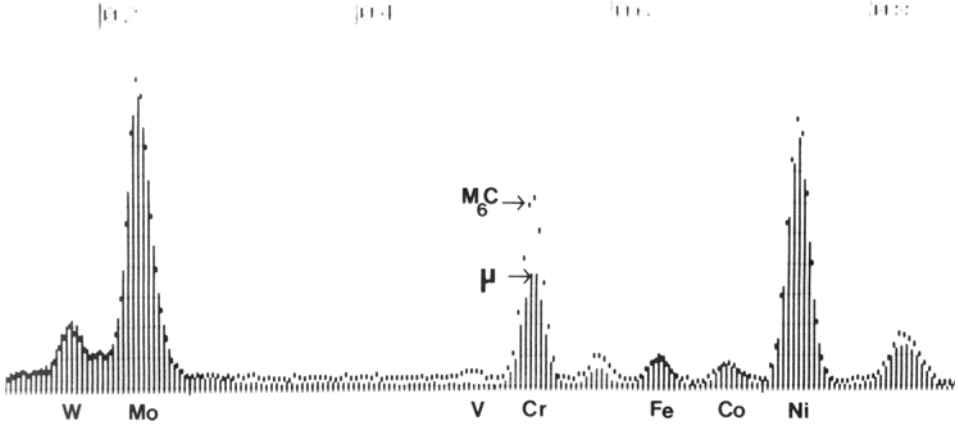

Fig. 5 — Superimposed X-ray spectra from the μ and M_6C carbide phases demonstrating the similarity in their compositions.

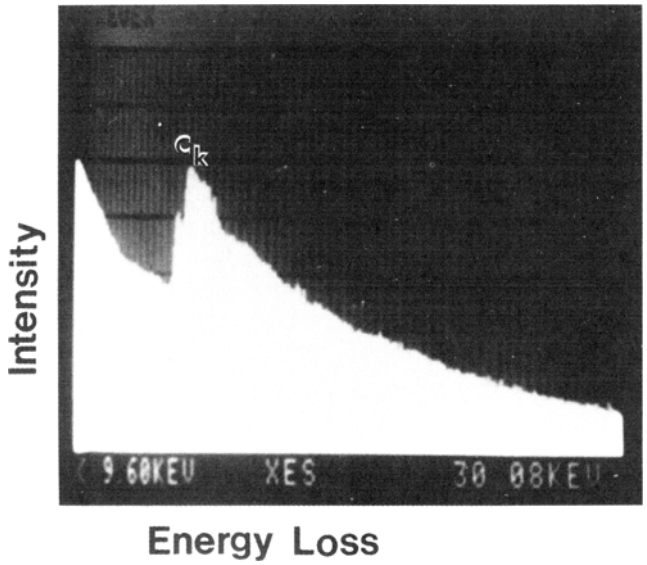

Fig. 6—Electron energy loss spectrum from an M_6C carbide particle showing the carbon absorption edge.

The least abundant second phase precipitates were tentatively identified as the *P* phase.[16,17] These particles were observed very infrequently and, like the carbides, did not contain any faults. Electron diffraction patterns from these particles could not be indexed either as a μ or M_6C phase but could be indexed based on a proposed tetragonal structure.[14]

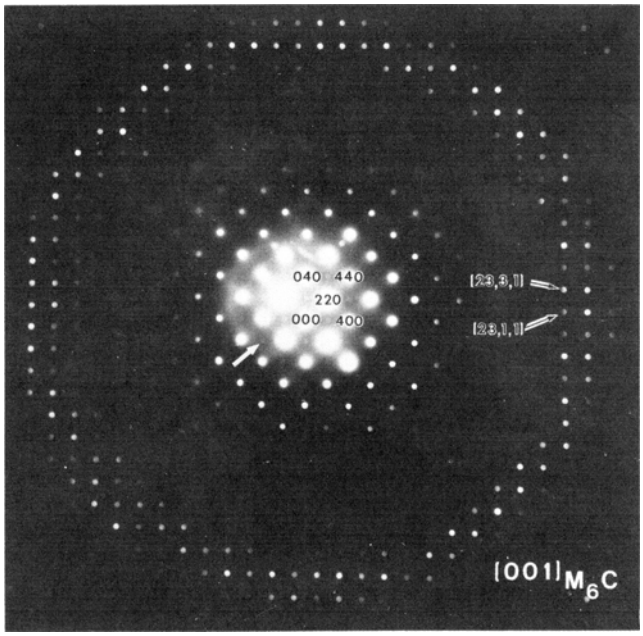

Fig. 8—A [001] microdiffraction pattern from an M_6C carbide showing the Zero and First Order Laue Zones. The arrow in the zero layer indicates weak reflection in the (200) type positions due to double diffraction.

Adequate zone axis diffraction patterns could not be generated from the *P* phase particles to identify positively their crystal structure. The X-ray microanalysis from a *P* phase

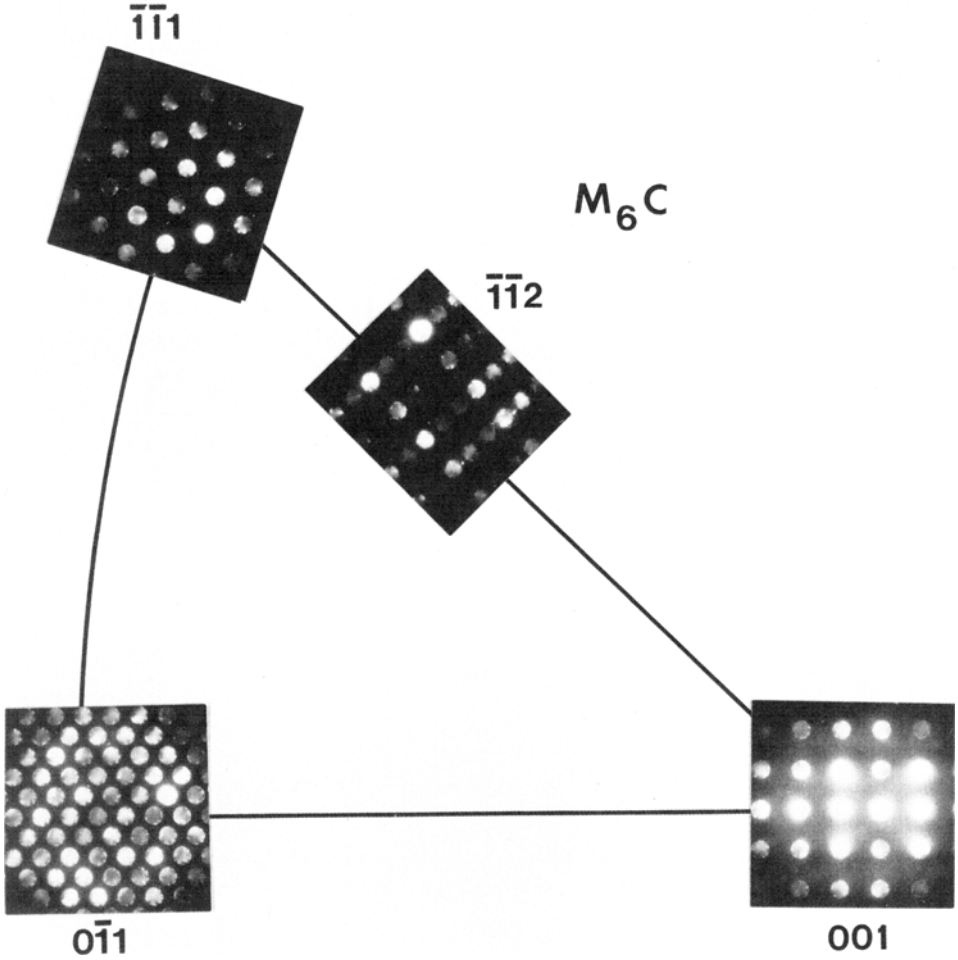

Fig. 7—Zone axis map of M_6C carbide.

particle is shown in Table II. Due to the limited number of P phase particles found in the alloy, errors are not specified. Again, the composition of this phase is very close to the composition of the M_6C and μ phases.

IV. DISCUSSION

An interesting result in the present analysis is that the composition of the μ phase is significantly different from the previous X-ray microprobe analysis of extracted residue reported by Hodge.[8] This difference can possibly be attributed to sample contamination introduced in the extraction procedures and subsequent errors in the analysis. Second phase particles in the range 500Å to 1 μm observed in the present investigation cannot be uniquely characterized by X-ray microprobe analysis of bulk samples alone. Extracts of the precipitates would be preferred for such analysis. However, in the presence of two or more precipitating phases, analysis of extracted residue could also lead to unambiguous results. In such cases, combination of X-ray microanalysis, microdiffraction, and electron energy loss analyses can be used to characterize unambiguously the structure and composition of the second phase particles.

The accuracy of X-ray microanalysis has been the subject of several previous investigations. It is interesting to note that the errors in analysis of the matrix (Table I) was lower than the errors in the analysis of precipitates (Table II). This could be due at least partly to the continuum generated during microanalysis which introduces X-ray contributions from regions outside the area analyzed. When the matrix is analyzed, the contribution from the other region in the sample may not cause serious errors since the matrix constitutes the major volume of the sample. Hence, errors in the matrix analysis are probably mostly due to counting statistics and other errors in measuring peak intensities and data handling such as absorption corrections, and so forth. However, in the analysis of the precipitates the extraneous contributions due to the continuum are primarily from the matrix due to its relative abundance. Since this contribution may vary from region to region, the errors involved in analyzing precipitates were larger. Nevertheless, the results showed that the analysis of the extracted precipitates compared well with the analysis of the precipitates in the thin sample and it is believed that the composition of the phases measured are accurate within the errors indicated.

As mentioned previously, μ phase is based on Fe-Mo alloy system with an A_7B_6 stoichiometry and substitution of Ni for Fe and Co is known to occur in the μ phase.[14] The μ phase composition in the present investigation can be written as $(Ni_{0.36}Cr_{0.16}Fe_{0.04}Co_{0.02})(Mo_{0.39}W_{0.03})$ which indicates extensive substitution of Ni and Cr for Fe and Co. This chemical formulation of the μ phase is different from the $(Ni, Co, Fe)_3(Mo, W, Cr)_2$ suggested by Kirchner and Hodge.[7] In order to obtain an Fe_7Mo_6 or Fe_3Mo_2 stoichiometry, the chromium should at least displace all or most of the iron atoms in the lattice. Since Ni_7Mo_6 or Cr_7Mo_6 compounds do not exist[23] in their respective binary systems, it is surprising that such an extensive substitution of Ni and Cr does occur in the μ phase. Van Loo, *et al*, have reported about 70 pct of the Fe in the μ phase can be replaced by nickel in the Fe-Ni-Mo ternary system.[20] The results of the present analysis also show that neither Fe nor Co selectively partition to the μ phase (Table II). The Fe content of the μ phase is actually less than the Fe content of the matrix while the cobalt levels of the matrix and μ phases are comparable. However, the formation of the phase in this alloy is dependent on the Fe and Co contents since it was shown that the μ phase did not form when the Fe and Co levels of the alloy were decreased to very low levels.[4] Thus, it is surprising that a compound based on Fe or Co based binary system should have such an extended solubility of Ni and Cr in the absence of isomorphous phases such as Ni_7Mo_6 and Cr_7Mo_6. In a recent publication, Kaufman and Nesor predicted that μ phase could form in Ni-Mo binary systems.[24] Though this may partly explain their present findings, there is no experimental evidence to support the prediction.

Since the compositions of the μ, M_6C, and P phases are remarkably close it is difficult to identify unambiguously these phases only by X-ray energy dispersive analysis in a SEM or in a STEM, and electron diffraction analysis was essential in identifying these phases. However, when the metal contents of these phases were compared, the carbides had about five pct higher chromium content than the μ and P phases and this difference can be used to identify preliminarily the carbides by X-ray microanalysis alone (Figure 5). The μ and P phases, however, could not be identified by chemical analysis alone. The closeness of P and μ phase compositions is not surprising since these are adjacent phases in the reported Fe-Ni-Mo ternary alloy systems.[20] Though it is possible that P phase is a transient phase decomposing to the stable μ phase upon prolonged aging as suggested by Leonard,[3] no direct evidence was observed to support this. The similarity of composition of the μ and M_6C phase appears coincidental.

The defect structure in the μ phase warrants further analysis since the streaking in the electron patterns cannot be totally attributed to the shape factor alone arising from the thin faults. Similar streaking effects have been observed previously by Dyson and Andrews in their diffraction analysis of faults in M_7C_3 carbides.[24] Further work is in progress to investigate this.

V. CONCLUSIONS

1. μ, M_6C, and P phases (in decreasing order of abundance) formed when Hastelloy C276 was aged in the temperature range of 923 to 1173 K.
2. These three phases were remarkably close in chemical composition. Microdiffraction analysis was essential to identify the phases.
3. The composition of μ phase is very rich in nickel and molybdenum, contrary to previously published reports.

REFERENCES

1. J.C. Scanlon, M. Raghavan, and B.J. Berkowitz: unpublished research, Exxon Research and Engineering Company, Linden, NJ, 1980.
2. R.B. Leonard: *Metals Progress*, 1971, vol. 99, p. 87.
3. R.B. Leonard: *Corrosion*, 1969, vol. 25, p. 222.
4. F.G. Hodge and R.W. Kirchner: *Corrosion*, 1976, vol. 32, p. 332.
5. R.W. Kirchner and W.L. Silence: *Materials Protection Performance*, 1971, vol. 10, p. 11.
6. C.H. Samans, A.R. Meyer, and G.F. Tisinai: *Corrosion*, 1966, vol. 22, p. 366.

7. R. W. Kirchner and F. G. Hodge: *Werkstoffe und Korrosion,* 1973, vol. 24, p. 42.
8. F. G. Hodge: *Corrosion,* 1973, vol. 29, p. 375.
9. M. A. Streicher: *Corrosion,* 1976, vol. 32, p. 79.
10. I. Class, H. Grafen, and E. Scheil: *Zeit. Metallkunde,* 1962, vol. 53, p. 283.
11. P. Johnson, Ph.D. Thesis, University of Notre Dame, 1980.
12. S. K. Das and G. Thomas: *Order-Disorder Transformations in Alloys,* H. Warlimont, ed., Springer-Verlag, New York, NY, 1974, p. 332.
13. M. Yamamoto, S. Nenno, T. Saburi, and Y. Mizutani: *Trans. JIM,* 1970, vol. 11, p. 120.
14. F. J. J. Van Loo, G. F. Bastin, J. W. G. A. Vrolijk, and J. J. M. Hendricks: *J. Less Common Metals,* 1980, vol. 72, p. 225.
15. H. J. Beattie, Jr. and W. C. Hagel: *Trans. TMS-AIME,* 1965, vol. 233, p. 227.
16. S. Rideout, W. D. Manly, E. L. Kamen, B. S. Lement, and P. A. Beck: *Trans. AIME,* 1951, vol. 191, p. 872.
17. D. S. Bloom and N. J. Grant: *J. Metals,* February 1954, p. 261.
18. G. Cliff and G. W. Lorimer: *J. Microscopy,* 1975, vol. 103, p. 203.
19. J. I. Goldstein: "Introduction to Analytical Electron Microscopy", J. J. Hren, J. I. Goldstein, and D. C. Joy, eds., Plenum Press, New York, NY, 1979, p. 83.
20. C. F. Klein and M. Raghavan: unpublished research, Exxon Research and Engineering Company, Linden, NJ, 1981.
21. J. W. Steeds: "Introduction to Analytical Electron Microscopy," J. J. Hren, J. I. Goldstein, and D. C. Joy, eds., Plenum Press, New York, NY, 1979, p. 387.
22. J. W. Steeds and N. S. Evans: *Proc. 38th Ann. Conf., Electron Microscopy Soc. Amer.,* G. W. Bailey, ed., Claitors Publishing Company, Baton Rouge, LA, 1980, p. 188.
23. M. Hansen: "The Constitution of Binary Alloys," McGraw Hill Co., New York, NY, 1958.
24. L. Kaufman and H. Nesor: *Metall. Trans.,* 1974, vol. 5, p. 1617.
25. D. J. Dyson and K. W. Andrews: *J. Iron Steel Inst.,* 1969, vol. 207, p. 208.